Transient Low-Affinity Agonist Binding to *Torpedo* Postsynaptic Membranes Resolved by Using Sequential Mixing Stopped-Flow Fluorescence Spectroscopy[†]

Douglas E. Raines* and Nanditha S. Krishnan

Department of Anesthesia and Critical Care, Massachusetts General Hospital, Boston, Massachusetts 02114

Received July 11, 1997; Revised Manuscript Received October 25, 1997

ABSTRACT: We have detected the binding of the fluorescent agonist Dns-C_6-Cho to both low- and high-affinity states of the nicotinic acetylcholine receptor (nAcChoR) using sequential mixing stopped-flow fluorescence spectroscopy. Our approach to resolving low- and high-affinity binding was to first preincubate receptor membranes with the fluorescent partial agonist Dns-C_6-Cho for 15 ms to 1000 s and then to follow the fluorescence decay upon chemical dilution into excess acetylcholine. The fast and slow decays, reflecting Dns-C_6-Cho dissociation from low- and high-affinity receptors, had rates of 140 ± 27 s^{-1} and 0.1 ± 0.02 s^{-1}, respectively. With increasing preincubation times, the number of low-affinity receptors decreased while the number of high-affinity receptors increased in a Dns-C_6-Cho concentration-dependent manner consistent with current models for agonist-induced affinity state conversion. At receptor-activating concentrations of Dns-C_6-Cho, the apparent rates with which high-affinity receptors formed approximated those of ion flux desensitization, implying that the fast desensitized state has an agonist dissociation rate that is indistinguishable from the equilibrium slow desensitized state. The K_D for the low-affinity binding site was determined to be 1.1 μM from the increase in the amplitude of the fast decay with Dns-C_6-Cho concentration with preincubation times that were sufficiently brief to minimize affinity state conversion. Assuming a bimolecular association rate of 10^8 M^{-1} s^{-1}, a second estimate of 1.4 μM was made for low-affinity binding. We also detected a fluorescence enhancement consistent with a conformational isomerization of Dns-C_6-Cho-inhibited nAcChoRs.

The nicotinic acetylcholine receptor (nAcChoR)[1] is a cation-selective ligand-gated ion channel that is found at the vertebrate neuromuscular junction and the electric organ of *Torpedo* (*1*, *2*). Electrophysiological (*3*, *4*) studies indicate that the binding of two agonist molecules rapidly leads to nAcChoR activation and ion flux. Agonists can also inhibit ion flux following channel opening, but this usually requires very high agonist concentrations (*5*−*7*). Prolonged exposure to agonist converts activated nAcChoRs first to a fast desensitized conformational state that is characterized by low ion permeability (*8*, *9*) and ultimately to an essentially impermeable slow desensitized state (*10*). The conversion of nAcChoRs to fast and slow desensitized states occurs on time scales of tens to hundreds of milliseconds and seconds to minutes, respectively.

Binding studies reveal that agonists also induce the nAcChoR to undergo a conformational conversion from a low-affinity state to one or more states of higher affinity (*11*, *12*). Such changes in agonist affinity are believed to be related to the permeability changes detected with electrophysiological and ion flux techniques (*10*, *13*). This has led to the development of a variety of kinetic models such as the one shown in Scheme 1 (*14*). In the absence of agonist, Scheme 1 considers the nAcChoR to exist in a conformational equilibrium between a low-affinity resting state (R) and a high-affinity desensitized state (D). Prior to agonist-induced conformational conversion, 80−90% of receptors are in the resting state and the remaining 10−20% are in the desensitized state. Agonist binding to low-affinity resting-state receptors rapidly converts them to the open channel state (A_2R^*) and ultimately to a set of closed, high-affinity desensitized states. Agonist may also bind to preexisting high-affinity desensitized receptors, but this does not lead to channel opening. Finally, agonists may bind to a site that is distinct from those which activate receptors, leading to blockade of the open channel (A_2R^*A). In most schemes describing nAcChoR conformational conversion, the rate of agonist binding to the activating sites on resting or desensitized nAcChoRs is considered to be at or near the limit of diffusion (*12*, *14*, *15*). Thus, the different agonist affinities exhibited by these two states are assumed to reflect their different agonist dissociation rates.

There is little direct data regarding the binding of agonist to nAcChoRs in the low-affinity conformational state. Radioligand binding studies have inadequate temporal resolution to define the kinetics of agonist binding to low-affinity nAcChoRs in detail because such receptors quickly isomerize to the high-affinity state (*11*). Although single mixing stopped-flow fluorescence techniques have significantly better temporal resolution, they have been unable to unambigu-

[†] This research was supported by a FIRST Award from the National Institute of General Medical Sciences (GM53481).

* Address correspondence to this author.

[1] Abbreviations: nAcChoR, nicotinic acetylcholine receptor; Dns-C_6-Cho, [1-[5-(dimethylamino)naphthalene]sulfonamido]-*n*-hexanoic acid β-(*N*-trimethylammonium bromide) ethyl ester; DFP, diisopropyl fluorophosphate; NBD-5-acylcholine, *N*-(7-nitro-2,1,3-benzoadiazol-4-yl)-5-aminopentanoic acid β-(*N*,*N*,*N*-trimethylammonium) ethyl ester; TPS, *Torpedo* physiological saline.

S0006-2960(97)01689-9 CCC: $15.00
Published on Web 01/01/1998

Scheme 1

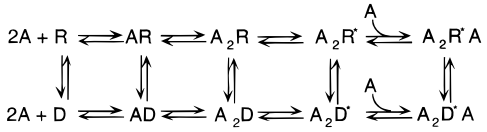

ously resolve agonist binding to sites of low affinity (*12*, *16*).

In this paper, we report the use of sequential mixing stopped-flow fluorescence spectroscopy to detect and characterize low- and high-affinity agonist binding to nAcChoRs. Our strategy was to preincubate nAcChoRs with the fluorescent agonist Dns-C_6-Cho and then to resolve agonist binding to low- and high-affinity receptor sites from the time course of Dns-C_6-Cho dissociation upon mixing with an excess of the nonfluorescent agonist acetylcholine; under conditions of energy transfer from nAcChoR tryptophan to Dns-C_6-Cho dansyl moiety, dissociation of Dns-C_6-Cho from nAcChoRs results in a reduction in fluorescence emission (*12*). Because our sequential mixing stopped-flow technique allows membranes to be preincubated with Dns-C_6-Cho for periods of time as brief as 15 ms prior to mixing with acetylcholine, Dns-C_6-Cho binding could be detected before the conformational equilibrium between low- and high-affinity receptor states could be significantly perturbed by the agonist. The Dns-C_6-Cho concentration dependence of the apparent rate of desensitization was determined by measuring the rate with which low-affinity receptors disappeared and high-affinity receptors appeared with longer preincubation times. An increase in fluorescence intensity was also observed with sequential mixing on an intermediate time scale (tens to hundreds of milliseconds) that we attribute to a conformational isomerization induced by Dns-C_6-Cho binding to the agonist inhibitory site. Our results are discussed in terms of current models describing nAcChoR activation and desensitization kinetics and a simple kinetic scheme is proposed to account for our data.

MATERIALS AND METHODS

Membrane Preparation and Characterization. Electric organs were obtained from *Torpedo nobiliana* (Biofish Associates, Georgetown, MA). Native membrane fragments were prepared by sucrose density gradient centrifugation at 4 °C as previously described and approved by the Massachusetts General Hospital Animal Care and Use Committee and stored in TPS at −80 °C. All membranes were used within 48 h of being thawed (*17*). The number of high-affinity agonist binding sites was determined from acetylcholine competition of (dansylaminoethyl)trimethylammonium perchlorate binding (*18*) and by equilibrium binding titrations using Dns-C_6-Cho (*12*). The number of binding sites determined with these two techniques typically differed by less than 25%. Acetylcholinesterase activity was inhibited by exposing concentrated membrane solutions to 1.0 mM DFP for 30−60 min. Membranes were then diluted to the desired concentration with TPS. Dns-C_6-Cho was synthesized as previously described (*19*).

Sequential Mixing Stopped-Flow Fluorescence Spectroscopy. Sequential mixing stopped-flow fluorescence experiments were performed using an Applied Photophysics SX.17MV stopped-flow spectrofluorometer (Leatherhead, U.K.). An excitation wavelength of 290 nm was provided by a 150 W xenon arc lamp. The monochromator's bandpass was set to 2.5 nm. Fluorescence was detected through a 530 nm high-pass filter on a logarithmic time base typically for either 10 or 100 s. The temperature was kept at 10.0 ± 0.2 °C with a circulator bath. In a typical experiment, 4−8 individual mixings were averaged to reduce noise. Averaged fluorescence traces were transferred to a Macintosh computer and analyzed using the commercially available analysis program Igor 3.0 (Wavemetrics Inc., Lake Oswego, OR).

In a typical experiment, receptor-rich membranes were loaded into one of the spectrofluorometer's premix syringes and a solution of Dns-C_6-Cho was loaded into the other. Receptor membranes and Dns-C_6-Cho were then rapidly mixed (1:1 v/v). After the desired preincubation period, the receptor membrane/Dns-C_6-Cho solution was rapidly mixed (1:1 v/v) with a solution containing 2 mM acetylcholine plus Dns-C_6-Cho at half the concentration present in the premix syringe to maintain a nearly constant free Dns-C_6-Cho concentration with the second mixing step. This second mixing step occurred within the optical cell where changes in fluorescence emission were recorded. The time axis on all stopped-flow fluorescence traces refers to the time after the second mixing. The reported nAcChoR and Dns-C_6-Cho concentrations are those during the preincubation period.

Computer simulations of Scheme 3 were performed by solving the differential equations by using the program SCIENTIST for Windows (Micromath, Salt Lake City, UT). For each simulation, the concentration of each conformational state was determined for the desired period of time following the mixing of nAcChoRs with Dns-C_6-Cho.

RESULTS

Figure 1A shows the slow fluorescence decay obtained when nAcChoR-rich membranes were preincubated with 2 μM Dns-C_6-Cho for either 200 s or 15 ms and then rapidly mixed with 1 mM acetylcholine. Fitting these decays between 1 and 50 s to an exponential equation yielded similar rates of 0.11 s^{-1} and 0.078 s^{-1} for membranes preincubated for 200 s and 15 ms, respectively. However, the amplitude of the slow decay was 10-fold larger in the trace obtained using receptor membranes preincubated for 200 s than in the trace obtained using membranes preincubated for 15 ms.

Figure 1B shows the same traces as in Figure 1A with the first 250 ms expanded for clarity. Two additional fluorescence components (a fast fluorescence decay and an intermediate enhancement in fluorescence) were observed on the subsecond time scale in the trace obtained using membranes that had been preincubated with Dns-C_6-Cho for 15 ms. These components were absent in membranes preincubated for 200 s. The fast fluorescence decay occurred on a time scale of 10 ms. The intermediate fluorescence enhancement occurred over several hundred milliseconds. The rates and amplitudes of these two components were determined by fitting the first second of the fluorescence trace to a double-exponential equation. The amplitude and rate of the fast fluorescence decay in this trace were 0.057 (arbitrary units) and 150 s^{-1}. The amplitude and rate of the intermediate fluorescence enhancement were 0.038 and 4.7 s^{-1}. Essentially identical values for the amplitudes and rates

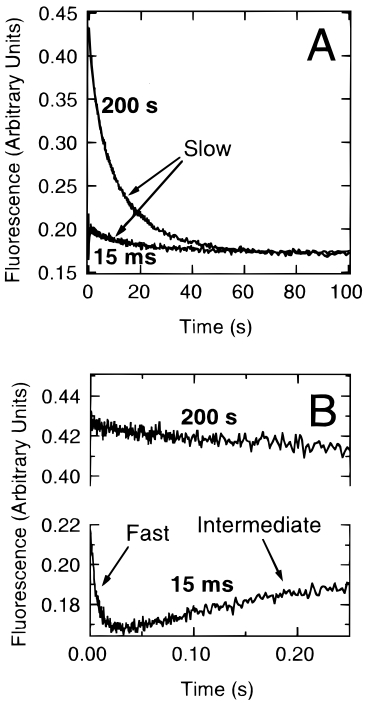

FIGURE 1: Panel A shows the change in fluorescence intensity recorded when nAcChoR membranes (0.4 μM agonist binding sites) that have been preincubated with 2 μM Dns-C_6-Cho for either 15 ms or 200 s are chemically diluted into 1 mM acetylcholine. The same traces are shown in panel B with the first 250 ms expanded to reveal the fast fluorescence decay and the intermediate fluorescence enhancement in membranes preincubated for 15 ms. The fast fluorescence decay and the intermediate fluorescence enhancement are absent in membranes preincubated for 200 s.

of all three fluorescence components (fast fluorescence decay, intermediate fluorescence enhancement, and slow fluorescence decay) were obtained by fitting all three fluorescence components to a triple-exponential equation. Preequilibrating membranes with the competitive antagonist α-bungarotoxin prior to sequential mixing (15 ms preincubation time) reduced the amplitudes of the fast and slow decays by more than 95% and that of the intermediate enhancement by 65% (data not shown). The three fluorescence components were further characterized as detailed below using sequential mixing stopped-flow fluorescence spectroscopy.

Slow Fluorescence Decay. Figure 2 shows typical fluorescence traces recorded when receptor membranes were preincubated for the indicated times with 2 μM Dns-C_6-Cho and then mixed with 1 mM acetylcholine. The rate of the slow fluorescence decay did not vary systematically with preincubation time and averaged 0.1 ± 0.02 s^{-1}. The amplitude of the slow decay increased with preincubation time before reaching a plateau by approximately 100 s. The inset in Figure 2 plots the amplitude of the decay as a function of preincubation time. The rate with which the amplitude of this decay increased with preincubation time (k_{slow}), determined by fitting the amplitude data in Figure 2 to an exponential equation, was 0.03 s^{-1}. A preincubation time-dependent increase in the amplitude of the slow decay was observed in studies using Dns-C_6-Cho concentrations ranging from 0.125 to 100 μM (Figure 3A). For all studies using Dns-C_6-Cho in excess over binding sites, the maximum amplitude reached after long preincubation times was independent of the Dns-C_6-Cho concentration and in the

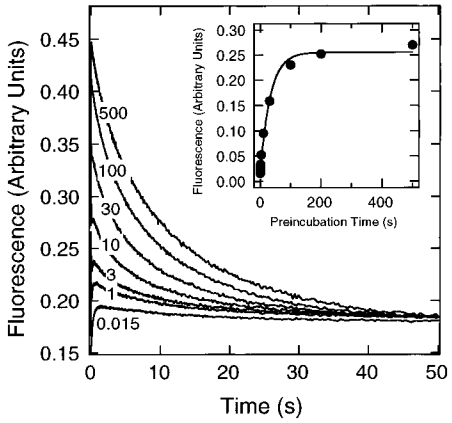

FIGURE 2: Change in fluorescence intensity recorded when nAcChoR membranes (0.4 μM agonist binding sites) that have been preincubated with 2 μM Dns-C_6-Cho for times ranging from 15 ms to 500 s are diluted into 1 mM acetylcholine. The amplitude of the slow decay increased with preincubation time (inset). The line is a fit of the amplitude data to a single-exponential equation yielding an apparent rate of 0.03 s^{-1}.

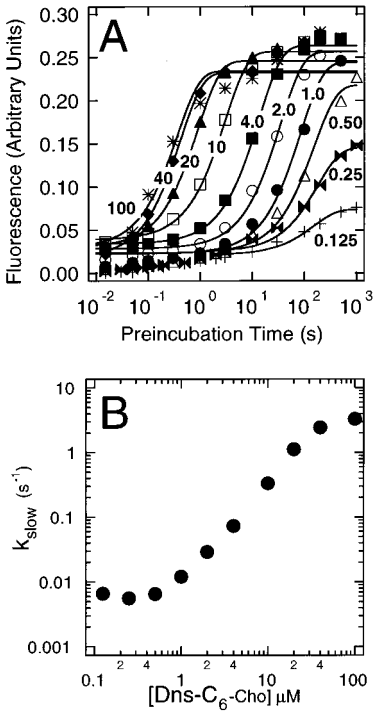

FIGURE 3: Panel A shows the increase in the amplitude of the slow decay with preincubation time. The following concentrations of Dns-C_6-Cho were used: (+) 0.125 μM, (double arrowheads) 0.25 μM, (△) 0.5 μM, (●) 1 μM, (○) 2 μM, (■) 4 μM, (□) 10 μM, (▲) 20 μM, (◆) 40 μM, and (*) 100 μM. For the 100 μM Dns-C_6-Cho titration, 10 mM rather than 1 mM acetylcholine was used in the second mixing step. The nAcChoR concentration was 0.4 μM in agonist binding sites. Panel B shows the values of k_{slow} (●) derived from exponential fits of the amplitude data in panel A.

membrane prep used to obtain the data in Figure 3 the amplitude ranged from 0.25 to 0.28. However, when Dns-C_6-Cho was not in excess over binding sites, the maximum amplitude was proportionately less.

At each Dns-C_6-Cho concentration, k_{slow} was determined by fitting the change in the amplitude of the slow decay to a single-exponential equation. A fraction of the increase in the amplitude of the slow fluorescence decay occurred on a slower (seconds to minutes) time scale at concentrations of

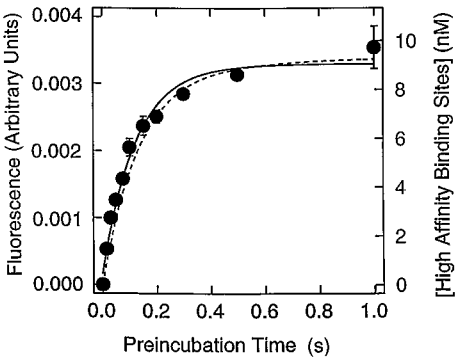

FIGURE 4: Small preincubation time-dependent increase in the amplitude of the slow decay on the subsecond time scale. The nAcChoR concentration was 0.1 μM in agonist binding sites and the Dns-C_6-Cho concentration was 0.25 μM. Data points are the average ±SD of three determinations using a single preparation. The solid line is a fit to an exponential equation yielding an apparent rate of 8 ± 0.95 s^{-1}. The dotted line shows the concentration of Dns-C_6-Cho bound to high-affinity desensitized nAcChoRs as a function of preincubation time determined from computer simulations of Scheme 3 using the parameters in Table 1.

Dns-C_6-Cho greater than 20 μM, but this was not included in the fit. The dependence of k_{slow} on Dns-C_6-Cho concentration is shown in Figure 3B. The limiting value of k_{slow} at low Dns-C_6-Cho concentrations was independent of Dns-C_6-Cho and equal to 0.006 s^{-1}. At Dns-C_6-Cho concentrations between 0.4 and 100 μM, k_{slow} increased by 550-fold to 3.3 s^{-1}.

Close inspection of Figure 3A also reveals that, at concentrations of Dns-C_6-Cho less than 2 μM, a small preincubation time-dependent increase in the amplitude of the slow decay on the subsecond time scale could be detected. This increase in amplitude was readily distinguished from k_{slow} because it was 100−1000 times faster, occurring on the time scale expected for Dns-C_6-Cho binding to preexisting high-affinity receptors. Figure 4 shows this increase in amplitude using a membrane concentration of 0.1 μM in binding sites and 0.25 μM Dns-C_6-Cho. An exponential fit of a plot of the amplitude as a function of preincubation time in this figure yielded an apparent rate of 8 ± 0.95 s^{-1}.

Fast Fluorescence Decay. Figure 5A shows a plot of the amplitude of the fast decay as a function of preincubation time with Dns-C_6-Cho concentrations ranging from 0.5 to 20 μM. Data are reported for Dns-C_6-Cho concentrations no higher than 20 μM because, above this, the fast decay could not be well resolved from the intermediate fluorescence enhancement (see next section). The rate of this decay did not vary systematically with either Dns-C_6-Cho concentration or preincubation time and averaged 140 ± 27 s^{-1}. At all Dns-C_6-Cho concentrations studied, the amplitude of the fast decay decreased with preincubation time. The rate with which the amplitude decreased with preincubation time (k_{fast}) was determined by fitting plots of the amplitude versus preincubation time to a single-exponential equation (Figure 5A). Over a concentration range from 0.5 to 20 μM, k_{fast} increased with Dns-C_6-Cho concentration from 0.011 s^{-1} to 1.2 s^{-1} (Figure 5B).

It is also apparent from the data in Figure 5A that, with short preincubation times (i.e., preincubation times that do not significantly reduce the amplitude of the fast decay), the amplitude of the fast decay increased and then plateaued with

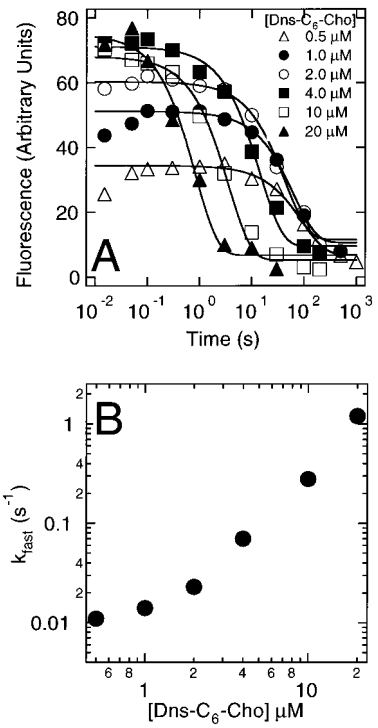

FIGURE 5: Panel A shows the increase in the amplitude of the fast decay with Dns-C_6-Cho preincubation time. Dns-C_6-Cho concentrations: (△) 0.5 μM, (●) 1 μM, (○) 2 μM, (■) 4 μM, (□) 10 μM, and (▲) 20 μM Dns-C_6-Cho. The nAcChoR concentration was 0.4 μM in agonist binding sites. Panel B shows the values of k_{fast} derived from exponential fits of the amplitude data in panel A.

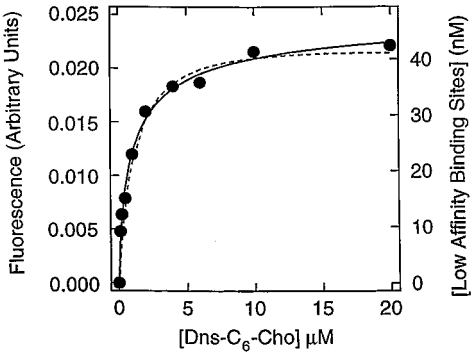

FIGURE 6: Amplitude of the fast fluorescence decay increases and then plateaus with Dns-C_6-Cho concentration. The concentration of nAcChoR was 0.1 μM in agonist binding sites and the preincubation time was 50 ms. The solid line is a fit of the data to eq 1 with K_{amp} equal to 1.1 ± 0.2 μM and a Hill coefficient equal to 0.7 ± 0.1. The dotted line is the concentration of Dns-C_6-Cho bound to the low-affinity site (K_D = 1.1 μM) on the nAcChoR resting state determined from computer simulations of Scheme 3 using the parameters in Table 1.

Dns-C_6-Cho concentration. Figure 6 shows a plot of the amplitude of the fast decay as a function of Dns-C_6-Cho concentration in a titration using a preincubation time of 50 ms. In this titration, a receptor concentration of 0.1 μM binding sites was used to minimize depletion of the free aqueous Dns-C_6-Cho concentration. The data were fit to

$$\mathrm{Amp} = \mathrm{Amp}_{max}\left(\frac{[\text{Dns-C}_6\text{-Cho}]^n}{[\text{Dns-C}_6\text{-Cho}]^n + K_{amp}{}^n}\right) \quad (1)$$

where Amp is the amplitude of the fast decay, Amp_{max} is

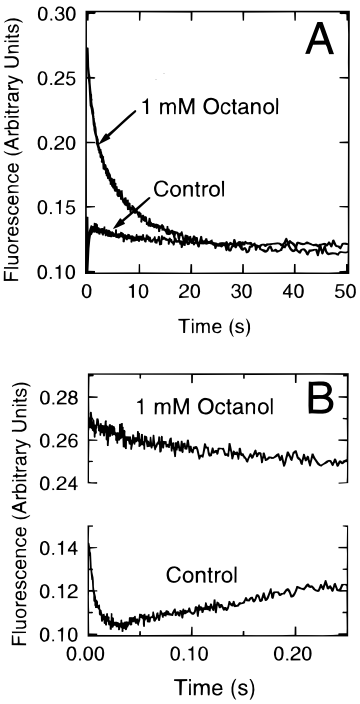

FIGURE 7: Panel A shows the effect of preequilibrating nAcChoR membranes with 1 mM octanol on sequential mixing stopped-flow fluorescence traces. Dns-C_6-Cho and nAcChoRs were preincubated for 15 ms. The nAcChoR concentration was 0.4 μM in agonist binding sites. The Dns-C_6-Cho concentration was 2 μM. The same traces are shown in panel B with the first 250 ms expanded to show that the fast fluorescence decay and the intermediate fluorescence enhancement are essentially eliminated by preequilibration of nAcChoRs with 1 mM octanol.

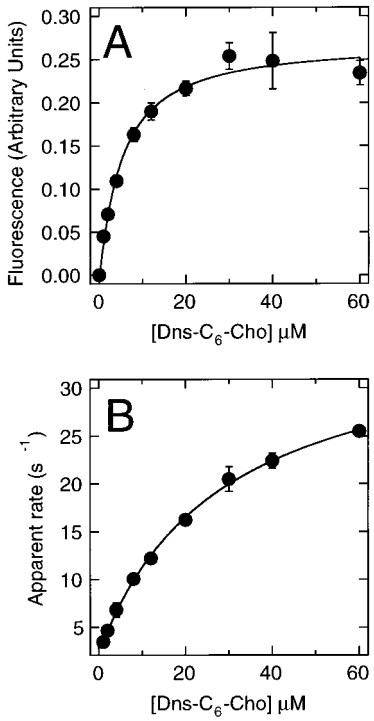

FIGURE 8: Amplitude of the intermediate fluorescence enhancement increases and plateaus with Dns-C_6-Cho (panel A). The curve is a fit to eq 1 with K_{amp} of 5.3 ± 0.9 μM and a Hill coefficient of 1.0 ± 0.1. The rate of the intermediate fluorescence enhancement increases in a nonlinear manner with Dns-C_6-Cho concentration (panel B). The value of K_D was 29 ± 3 μM, k_2 was 34 ± 1 s^{-1}, and k_{-2} was 2.5 ± 0.2 s^{-1}. The preincubation time was 15 ms. The nAcChoR concentration was 0.4 μM in agonist binding sites. Data points are the average ±SD of three determinations using a single preparation.

the maximal amplitude reached at high Dns-C_6-Cho concentrations, n is the Hill coefficient, and K_{amp} is the Dns-C_6-Cho concentration at which the amplitude is half-maximal. The value of K_{amp} was determined to be 1.1 ± 0.2 μM and the Hill coefficient was 0.7 ± 0.1.

We examined the effect of preequilibrating nAcChoR membranes with 1 mM octanol using a preincubation time of 50 ms. Octanol is a noncompetitive inhibitor of nAcChoR that stabilizes the desensitized conformation of nAcChoR (*20*). To keep the concentration of octanol constant upon sequential mixing, 1 mM octanol was also added to the Dns-C_6-Cho and acetylcholine solutions where appropriate. Panels A and B of Figure 7 show fluorescence traces from control membranes (no octanol) and from membranes that had been preequilibrated with 1 mM octanol, respectively. Octanol reduced the amplitude of the fast decay (and the intermediate enhancement) to immeasurable levels. Conversely, it increased the amplitude of the slow decay from 0.014 to 0.15. Similarly, preequilibrating membranes (0.1 μM binding sites) with Dns-C_6-Cho (0.15 μM) prior to sequential mixing with a 15 ms preincubation time completely eliminated the fast decay (and intermediate enhancement).

Intermediate Fluorescence Enhancement. In addition to the two fluorescence decays detected on the millisecond and second time scales, an increase in fluorescence intensity was observed in experiments using short preincubation times. The amplitude of this fluorescence component was reduced or eliminated by using long preincubation times (see Figure 1, 200 s preincubation time). In experiments using a 15 ms preincubation time, the amplitude of this fluorescence enhancement increased with Dns-C_6-Cho concentration before plateauing at approximately 20 μM (Figure 8A). A fit of the amplitude data of eq 1 yielded a K_{amp} of 5.3 ± 0.9 μM and a Hill coefficient of 1.0 ± 0.1. The observed rate of this process increased with Dns-C_6-Cho concentration in a nonlinear manner, indicating that this was not a simple bimolecular binding reaction (Figure 8B). The data may be accounted for by a simple kinetic scheme in which rapid binding of Dns-C_6-Cho to nAcChoRs induces a slower conformational isomerization as shown in Scheme 2, where L is Dns-C_6-Cho, P is nAcChoR, and the conformational isomerization of LP to LP′ results in the fluorescence enhancement. The kinetic constants given in Scheme 2 can be derived from the observed rate of the fluorescence enhancement using (*21*)

$$k_{obs} = \frac{k_f}{1 + \frac{K_D}{[\text{Dns-C}_6\text{-Cho}]}} + k_b \qquad (2)$$

From the data in Figure 8A, we obtained values of 29 ± 3 μM for K_D, 34 ± 1 s^{-1} for k_f, and 2.5 ± 0.2 s^{-1} for k_b.

Scheme 2

$$L + P \overset{K_D}{\rightleftharpoons} LP \underset{k_b}{\overset{k_f}{\rightleftharpoons}} LP'$$

When the nonfluorescent competing agonists were used at very high concentrations, the amplitude of the intermediate

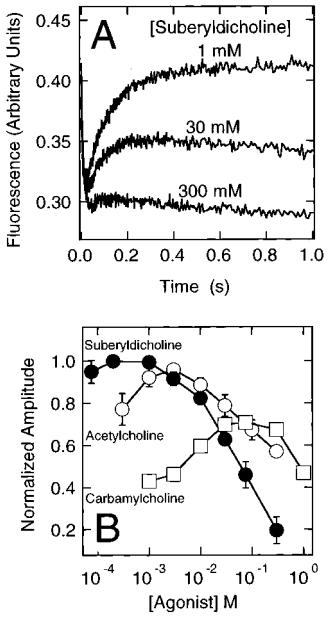

FIGURE 9: At high concentrations of suberyldicholine, the amplitude of the intermediate fluorescence enhancement is reduced (panel A). The amplitude of the intermediate fluorescence enhancement exhibits a bell-shaped dependence on the concentration of competing nonfluorescent agonist (panel B). (●) Suberyldicholine; (○) acetylcholine; (□) carbamylcholine. The amplitudes were normalized to that obtained with 200 μM suberyldicholine. The preincubation time was 15 ms. The nAcChoR concentration was 1.6 μM in agonist binding sites. The concentration of Dns-C_6-Cho was 10 μM. Data points are the average ±SD of three determinations using a single preparation.

fluorescence enhancement was reduced (Figure 9A). These concentrations did not alter the amplitudes of the fast or slow decays. Figure 9B shows the variation in the amplitude of the intermediate fluorescence enhancement with three different competing nonfluorescent agonists over a wide range of agonist concentrations. To facilitate comparisons among agonists, the amplitudes have been normalized to that obtained with 200 μM suberyldicholine. Concentrations of nonfluorescent agonist lower than those shown in this figure did not fully compete with Dns-C_6-Cho for agonist binding sites as evidenced by a slow increase in fluorescence intensity similar to that reported for single mixing experiments. The maximum amplitudes obtained with suberyldicholine and acetylcholine were not different, while that obtained with carbamylcholine was 30% lower. The concentration of agonist required to obtain the maximal amplitude varied with agonist, being lowest for suberyldicholine (200 μM), intermediate for acetylcholine (3 mM), and highest for carbamylcholine (75 mM). Increasing the nonfluorescent agonist concentrations above these concentrations resulted in a reduction in the amplitude of this component without significantly altering the amplitudes of the fast or slow decays (Figure 9B).

DISCUSSION

Typical models of nAcChoR affinity state conversion consider two populations of receptors to be present prior to agonist-induced affinity state conversion that may be distinguished by their agonist dissociation rates. Within the context of such models, the fluorescence decays that we observe on fast and slow time scales with rapid sequential mixing are most economically attributed to competitive displacement of the fluorescent agonist Dns-C_6-Cho by acetylcholine from the low-affinity resting and the high-affinity desensitized conformational states, respectively. Our assignment of the fast and slow decays to agonist dissociation from the nAcChoR resting and desensitized states in Scheme 1 is supported by the following experimental observations: (1) desensitizing nAcChoRs by preincubating membranes with Dns-C_6-Cho for several minutes eliminated the fast decay and increased the amplitude of the slow decay by 10-fold, (2) preequilibrating nAcChoRs with a desensitizing concentration of octanol eliminated the fast fluorescence decay and increased the amplitude of the slow decay, and (3) preequilibrating nAcChoRs with the competitive antagonist α-bungarotoxin prior to sequential mixing experiments eliminated both fast and slow decays.

Because agonist binding and channel gating kinetics in nAcChoRs are fast relative to affinity state transitions (*11*, *14*, *22*, *23*), all R states depicted in Scheme 1 are in a pseudoequilibrium on the time scale of desensitization. Assuming that these low-affinity receptors isomerize directly to the high-affinity state, the rate with which agonist-bound resting state low-affinity sites disappear (k_{fast}) and agonist-bound high-affinity desensitized state sites appear (k_{slow}) should be equal. Comparison of Figure 3B with Figure 5B reveals that, at equal Dns-C_6-Cho concentrations, these rates are, in fact, essentially identical. Both k_{fast} and k_{slow} increase with Dns-C_6-Cho concentration. Of note, the highest value determined for k_{slow} is 3.3 s^{-1}, which is at least an order of magnitude faster than the rate of slow desensitization previously determined using agonist binding or ion flux studies (*9*, *10*, *12*) and approximates the 2−7 s^{-1} reported for the rate constant for fast desensitization (*6*, *7*, *9*). This implies that the fast desensitized conformational state detected with ion flux techniques has an agonist dissociation rate that is similar, if not identical, to that of the equilibrium slow desensitized state. In experiments using high concentrations of Dns-C_6-Cho, we did resolve a preincubation time-dependent increase in the slow fluorescence decay that occurred over a seconds to minutes time scale, perhaps related to the process of slow desensitization.

The association rate constant of Dns-C_6-Cho to preexisting high-affinity nAcChoRs was determined by using relatively low concentrations of both Dns-C_6-Cho and nAcChoR (0.1 and 0.25 μM sites, respectively). Under these conditions, the time course of Dns-C_6-Cho binding could be followed with sequential mixing as a preincubation time-dependent increase in the amplitude of the slow decay on the subsecond time scale (Figure 4). The amplitude of the slow decay increased with an apparent rate of 8 ± 0.95 s^{-1}. Assuming pseudo-first-order binding of Dns-C_6-Cho to preexisting high-affinity receptors, we calculate an association rate constant of 3×10^7 M^{-1} s^{-1}. An identical value has been reported for acetylcholine binding (*11*). Heidmann and Changeux reported a value for Dns-C_6-Cho binding to high-affinity nAcChoRs that was 3 times faster than our estimate (*12*). In their studies, the Dns-C_6-Cho association rate constant was determined from a plot of the apparent rate of a rapid binding process observed in single mixing stopped-flow fluorescence traces as a function of Dns-C_6-Cho concentration. However, our sequential mixing experiments reveal that at the concentrations they used to derive their association rate constant,

Dns-C_6-Cho binds rapidly to two classes of binding sites that can be distinguished by their different agonist dissociation rates. Thus, apparent binding rates determined with single mixing stopped-flow fluorescence spectroscopy using micromolar concentrations of Dns-C_6-Cho reflect a composite rate of binding to nAcChoR sites of high and low affinity.

Kinetic modeling of the binding of NBD-5-acylcholine to *Torpedo* nAcChoR membranes (*15*) and analyses of single-channel currents from cloned *Torpedo* receptors (*4*) indicate that the K_Ds of the two resting state agonist binding sites differ by 2−3 orders of magnitude. It has been suggested that this large difference in affinity is required for rapid activation and termination of nAcChoR (*24*). The K_D of Dns-C_6-Cho for the low-affinity site detected in our study was determined from the increase in the amplitude of the decay with Dns-C_6-Cho concentration. Provided that the preincubation time is sufficient to allow binding to preexisting low-affinity nAcChoRs to reach equilibrium without perturbing the preexisting affinity state equilibrium (i.e., 50 ms) and depletion of the free Dns-C_6-Cho is minimal, the amplitude of the fast decay will increase with Dns-C_6-Cho concentration before plateauing. The Dns-C_6-Cho concentration producing a half-maximal amplitude (1.1 μM) will be equal to the K_D for the low-affinity site (Figure 6). If we assume that the association constant is at or near the limit of diffusion ($\sim 10^8$ M^{-1} s^{-1}), then we can derive a second estimate of the K_D equal to 1.4 μM from the dissociation rate constant of 140 s^{-1}. These values are similar to the K_Ds estimated for acetylcholine (*4*) and NBD-5-acylcholine (*15*) binding to the resting state site having the higher affinity for agonist (4.2 μM and 1.7 μM, respectively). This suggests that the quaternary ammonium moiety is the principal determinant of an agonist's affinity for this site. We do not detect agonist binding to the other (very low affinity) resting state site. This is not unexpected because Dns-C_6-Cho would probably dissociate from a very low affinity site wiithin the 1 ms dead time of our spectrofluorometer (*4*). However, we can infer from our data that a very low affinity resting state site probably does exist because the apparent rate of affinity state conversion increases steadily up to high Dns-C_6-Cho concentrations.

In addition to binding to the two activating sites, agonists also bind to a site on the open state, leading to ion flux inhibition (*5*−*7*). In this way, agonists may act as channel blockers as well as activators. For most agonists, the apparent K_D for self-inhibition is much greater than that for the activation. For example, the apparent K_D for acetylcholine inhibition in the absence of a transmembrane potential is on the order of 10 mM while that for activation is only 100 μM (*5*). Consequently, flux−response curves using acetylcholine are bell-shaped. Similarly, suberyldicholine and carbamylcholine have bell-shaped flux−response curves (*5*). However, some agonists have apparent K_Ds for self-inhibition that are either similar to or less than that for activation and therefore induce a maximal flux that is less than that achieved with full agonists such as acetylcholine (*25*, *26*). Additionally, some agonists induce a low level of flux because they have an intrinsically low efficacy (*27*). Rapid quench−flow studies reveal that Dns-C_6-Cho induces a relatively low level of flux across nAcChoR-rich membranes (*13*). Because Dns-C_6-Cho blocks the flux induced by saturating concentrations of acetylcholine with an apparent K_D of 24 μM (*28*), it is clear that, in addition to being an agonist, Dns-C_6-Cho is also a potent open channel blocker.

Scheme 3

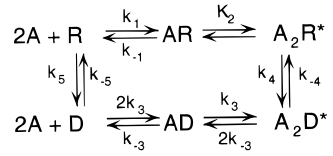

In our sequential mixing experiments, we observe an enhancement in fluorescence intensity on a time scale of tens to hundreds of milliseconds upon mixing 1 mM acetylcholine with receptors that have been briefly preincubated with Dns-C_6-Cho. Because 1 mM acetylcholine not only competes with Dns-C_6-Cho for binding to nAcChoR activating sites but also rapidly opens channels without inhibiting them, it seems reasonable to consider that this fluorescence enhancement might result from Dns-C_6-Cho binding to the agonist self-inhibitory site following channel activation. However, the observed rate of the fluorescence enhancement is almost certainly too slow to represent the binding event itself because such binding must occur within a millisecond to account for the low level of flux induced by Dns-C_6-Cho and its ability to block acetylcholine-induced flux. Additionally, the observed rate increases hyperbolically rather than linearly with Dns-C_6-Cho concentration. Conversely, our data are consistent with a conformational conversion induced by the rapid binding of Dns-C_6-Cho to the open state self-inhibitory site (Scheme 2). An analogous model has been used to account for the fluorescence enhancement seen when agonists are mixed with *Torpedo* membranes that have been preincubated with the fluorescent noncompetitive inhibitors ethidium (*29*) or quinicrine (*30*): the inhibitor rapidly binds to a site on the open channel state and a fluorescence enhancement is observed upon isomerization of the inhibitor−nAcChoR complex. In support of our assignment, the 29 μM K_D of Dns-C_6-Cho for the inhibitory site derived from the observed rate of the fluorescence enhancement is similar to the concentration of Dns-C_6-Cho that reduces acetylcholine-induced flux by half. Our assignment predicts that octanol (or long preincubation times) would reduce or eliminate the intermediate fluorescence enhancement simply because desensitized channels do not open in response to 1 mM acetylcholine. The bell-shaped amplitude−agonist concentration curves in Figure 9A can then be explained in terms of two processes: (1) At low (channel-activating) concentrations, the nonfluorescent agonist increases the fraction of receptors that reach the Dns-C_6-Cho-inhibited open state, and (2) at high (channel inhibiting) concentrations, the nonfluorescent agonist competes effectively with Dns-C_6-Cho for the inhibitory site and there is little formation of the Dns-C_6-Cho−nAcChoR complex.

Because all 28 rate constants that define Scheme 1 have not been determined, it is not possible to completely and accurately simulate the kinetics of Dns-C_6-Cho binding, dissociation, desensitization, and inhibition. However, a simplified version of Scheme 1 may be used to test our assignment of the slow and fast decays to Dns-C_6-Cho dissociation from high- and low-affinity nAcChoRs (Scheme 3). According to Scheme 3, the binding of Dns-C_6-Cho to two low-affinity resting state sites having different agonist affinities leads to nAcChoR desensitization. Agonist also

Table 1: Equilibrium and Rate Constants for Simulation of Scheme 3

equilibrium and rate constants	value	determination
K_1	1.1×10^{-6} M	concentration dependence on the fast decay amplitude with 50 ms preincubation time
k_{-1}	140 s^{-1}	rate of the fast decay
k_1	1.3×10^8 M^{-1} s^{-1}	$k_1 = k_{-1}/K_1$
K_2	1×10^{-4} M	apparent affinity for Dns-C_6-Cho-induced ion flux and desensitization[a]
K_3	3×10^{-9} M	$K_3 = k_{-3}/k_3$
k_{-3}'	0.1 s^{-1}	rate of the slow decay
k_3'	3×10^7 M^{-1} s^{-1}	rapid increase in the amplitude of the slow decay at low [Dns-C_6-Cho] and [nAcChoR]
K_5	10	amplitude of the slow decay with long preincubation times (equilibrium) divided by its amplitude after short preincubation times
k_{-5}	5×10^{-3} s^{-1}	Dns-C_6-Cho independent value of k_{slow} at low [Dns-C_6-Cho] equals $k_{-5} + k_5$
k_5	5×10^{-4} s^{-1}	$k_5 = k_{-5}/K_5$
k_4	7 s^{-1}	rate constant for ion flux desensitization[b]
k_{-4}	7.22×10^{-6} s^{-1}	thermodynamic constraint

[a] From quench-flow studies using Dns-C_6-Cho at 20 °C (*13*). For the purpose of simulating our data, the association (k_2) and dissociation (k_{-2}) rate constants that determine K_2 are assumed to be 10^8 M^{-1} s^{-1} and 10^4 s^{-1}. [b] Estimated value for *Torpedo nobiliana* are from ion flux studies using acetylcholine at 4 °C (*6*).

binds to two high-affinity sites on the desensitized state, but these sites are indistinguishable. Our data indicate that desensitization from the singly liganded state is negligible because 1 μM Dns-C_6-Cho does not substantially increase the apparent rate of affinity state conversion of resting state receptors to the desensitized state over that rate induced by limitingly low Dns-C_6-Cho concentrations. In contrast to Scheme 1, Scheme 3 considers A_2R, A_2R^0, and A_2RA together as A_2R^* because transitions between these states are fast on the time scale of our fluorescence technique. For simplicity, this scheme also considers receptor states A_2D, A_2D^0, and A_2DA together as A_2D^* (*31*, *32*). Finally we have assumed that the rate constant for Dns-C_6-Cho-induced desensitization is not significantly different from the $\sim$7 s^{-1} rate reported for acetylcholine-induced ion flux desensitization in *Torpedo nobiliana* (*6*, *32*).

Our assignment of the slow fluorescent to Dns-C_6-Cho dissociation from high-affinity sites in Scheme 3 requires that the amplitude of the slow decay be proportional to the concentration of Dns-C_6-Cho bound to AD and A_2D. Similarly, our assignment of the fast fluorescent decay to Dns-C_6-Cho dissociation from low-affinity sites implies that the amplitude of the fast decay will be proportional to the concentration of Dns-C_6-Cho bound to both AR and the higher affinity site of ARA. With the parameters in Table 1, computer simulations of Scheme 3 were used to derive the concentrations of Dns-C_6-Cho bound to these high- and low-affinity sites as a function of preincubation time with

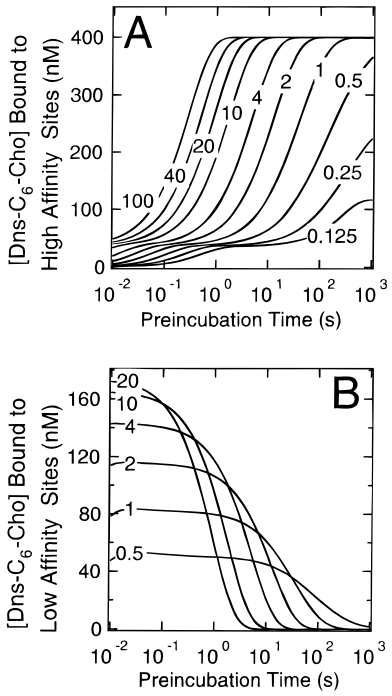

FIGURE 10: Computer simulations of Scheme 3 using the parameters in Table 1. Panel A shows the concentrations of Dns-C_6-Cho bound to two high-affinity sites on receptors in the densensitized state as a function of Dns-C_6-Cho preincubation time. Panel B shows the concentrations of Dns-C_6-Cho bound to a 1.1 μM K_D site on receptors in the resting state as a function of Dns-C_6-Cho preincubation time. The concentration of Dns-C_6-Cho (micromolar) is indicated in each panel. The concentration of nAcChoRs was 0.4 μM in equilibrium high-affinity sites.

Dns-C_6-Cho (Figure 10). Considering the simplicity of Scheme 3, these figures mirror the experimental amplitude data shown in Figures 3A and 5A reasonably well. Similarly, the simulations agree well with the experimental binding data shown in Figures 4 and 6.

In conclusion, we have used sequential mixing stopped-flow fluorescence spectroscopy to resolve agonist binding to both low- and high-affinity states of nAcChoR. The fluorescent agonist Dns-C_6-Cho binds to a high-affinity state with a K_D of 3 nM. Dns-C_6-Cho also binds to a transient low-affinity site with a K_D of approximately 1 μM. In agreement with current models of nAcChoR desensitization, prolonged exposure of receptors to agonist reduces the number of low-affinity binding sites and increases the number of high-affinity sites with apparent rates that increase with agonist concentration. At high agonist concentrations, the apparent rate with which high-affinity sites appeared corresponded to those reported for fast desensitization of flux response, suggesting that the fast desensitized state has an agonist dissociation rate that is similar to that of the equilibrium (slow) desensitized state. We also observed an enhancement in fluorescence intensity on a time scale of tens to hundreds of milliseconds with the sequential mixing technique that may reflect a conformational isomerization following Dns-C_6-Cho binding to the nAcChoR's agonist self-inhibitory site.

ACKNOWLEDGMENT

We thank Dr. S. Shaukat Husain for synthesizing Dns-C_6-Cho.

APPENDIX

Differential equations used for simulations of Scheme 3 were as follows:

$$dR/dt = k_{-5}[D] - k_5[R] + k_{-1}[AR] - k_1[R][A]$$

$$dAR/dt = k_1[R][A] - k_{-1}[AR] + k_{-2}[A_2R^*] - k_2[AR][A]$$

$$dA_2R^*/dt = k_2[AR][A] - k_{-2}[A_2R^*] + k_{-4}[A_2D^*] - k_4[A_2R^*]$$

$$dA_2D^*/dt = k_4[A_2R^*][A] - k_{-4}[A_2D^*] + k_3[AD][A] - 2k_{-3}[A_2D^*]$$

$$dAD/dt = 2k_3[D][A] - k_{-3}[AD] + 2k_{-3}[A_2D^*] - k_3[AD][A]$$

$$dD/dt = k_5[R] - k_{-5}[D] + k_{-3}[AD] - 2k_3[D][A]$$

$$dA/dt = k_{-1}[AR] - k_1[R][A] - k_2[AR][A] - k_{-2}[A_2R^*] - 2k_3[D][A] + k_{-3}[AD] - k_3[AD][A] + 2k_{-3}[A_2D^*]$$

REFERENCES

1. Lingle, C. J., Maconochie, D., and Steinbach, J. H. (1992) *J. Membr. Biol. 126*, 195−217.
2. Stroud, R. M., McCarthy, M. P., and Shuster, M. (1990) *Biochemistry 29*, 11009−11023.
3. Jackson, M. B. (1988) *J. Physiol. 397*, 555−583.
4. Sine, S. M., Claudio, T., and Sigworth, F. J. (1990) *J. Gen. Physiol. 96*, 395−437.
5. Forman, S. A., Firestone, L. L., and Miller, K. W. (1987) *Biochemistry 26*, 2807−2814.
6. Forman, S. A., and Miller, K. W. (1988) *Biophys. J. 54*, 149−158.
7. Takeyasu, K., Shiono, S., Udgaonkar, J. B., Fujita, N., and Hess, G. P. (1986) *Biochemistry 25*, 1770−1776.
8. Feltz, A., and Trautmann, A. (1982) *J. Physiol. 322*, 257−272.
9. Walker, J. W., Takeyasu, K., and McNamee, M. G. (1982) *Biochemistry 21*, 5384−5389.
10. Neubig, R. R., Boyd, N. D., and Cohen, J. B. (1982) *Biochemistry 21*, 3460−3467.
11. Boyd, N. D., and Cohen, J. B. (1980) *Biochemistry 19*, 5344−5353.
12. Heidmann, T., and Changeux, J. P. (1979) *Eur. J. Biochem. 94*, 255−279.
13. Heidmann, T., Bernhardt, J., Neumann, E., and Changeux, J. P. (1983) *Biochemistry 22*, 5452−5459.
14. Dilger, J. P., and Liu, Y. (1992) *Pflugers Arch. 420*, 479−485.
15. Prinz, H., and Maelicke, A. (1992) *Biochemistry 31*, 6728−6738.
16. Heidmann, T., and Changeux, J. P. (1980) *Biochem. Biophys. Res. Commun. 97*, 889−896.
17. Braswell, L. M., Miller, K. W., and Sauter, J. F. (1984) *Br. J. Pharmacol. 83*, 305−311.
18. Neubig, R. R., and Cohen, J. B. (1979) *Biochemistry 18*, 5464−5475.
19. Waksman, G., Fournie, Z. M. C., and Roques, B. (1976) *FEBS Lett. 67*, 335−342.
20. Firestone, L. L., Alifimoff, J. K., and Miller, K. W. (1994) *Mol. Pharmacol. 46*, 508−515.
21. Christensen, U., and Molgaard, L. (1991) *FEBS Lett. 278*, 204−206.
22. Liu, Y., and Dilger, J. P. (1991) *Biophys. J. 60*, 424−432.
23. Sine, S. M., and Steinbach, J. H. (1987) *J. Physiol. 385*, 325−359.
24. Jackson, M. B. (1989) *Proc. Natl. Acad. Sci. U.S.A. 86*, 2199−2203.
25. Johnson, D. A., Brown, R. D., Herz, J. M., Bermann, H. A., Andreasen, G. L., and Taylor, P. (1987) *J. Biol. Chem. 262*, 14022−14029.
26. Tonner, P. H., Wood, S. C., and Miller, K. W. (1992) *Mol. Pharmacol. 42*, 890−897.
27. Liu, Y., and Dilger, J. P. (1993) *Synapse 13*, 57−62.
28. Rankin, S. E. (1995) in *Biological Sciences*, p 166, Oxford University, Oxford, U.K.
29. Quast, U., Schimerlik, M. I., and Raftery, M. A. (1979) *Biochemistry 18*, 1891−1901.
30. Grunhagen, H. H., Iwatsubo, M., Changeux, J. P. (1977) *Eur. J. Biochem. 80*, 225−242.
31. Colquhoun, D., and Ogden, D. C. (1988) *J. Physiol. 395*, 131−159.
32. Wu, G., and Miller, K. W. (1994) *Biochemistry 33*, 9085−9091.

BI971689W